AGU PUBLICATIONS

Geophysical Research Letters

RESEARCH LETTER
10.1002/2017GL076575

Key Points:
- Plumes developing in a visco-plastic fluid present much larger diameters than plumes developing in a Newtonian fluid
- Such a rheology requiring a yield stress is consistent with a lower mantle predominantly deforming by pure dislocation climb
- This deformation mechanism could explain the morphology of plumes in the lower mantle recently imaged by seismic tomography

Correspondence to:
A. Davaille,
davaille@fast.u-psud.fr

Citation:
Davaille, A., Carrez, P., & Cordier, P. (2018). Fat plumes may reflect the complex rheology of the lower mantle. *Geophysical Research Letters*, *45*, 1349–1354. https://doi.org/10.1002/2017GL076575

Received 3 DEC 2017
Accepted 26 JAN 2018
Accepted article online 5 FEB 2018
Published online 12 FEB 2018

Fat Plumes May Reflect the Complex Rheology of the Lower Mantle

A. Davaille[1], Ph. Carrez[2], and P. Cordier[2]

[1]Laboratoire FAST, CNRS/University of Paris-Sud/University of Paris-Saclay, Orsay, France, [2]University of Lille, INRA, ENSCL, UMR 8207-UMET-Unite Materiaux et Transformations, Lille, France

Abstract Recent tomographic imaging of the mantle below major hot spots shows slow seismic velocities extending down to the core-mantle boundary, confirming the existence of mantle plumes. However, these plumes are much thicker than previously thought. Using new laboratory experiments and scaling laws, we show that thermal plumes developing in a visco-plastic fluid present much larger diameters than plumes developing in a Newtonian fluid. Such a rheology requiring a yield stress is consistent with a lower mantle predominantly deforming by pure dislocation climb. Yield stress values between 1 and 10 MPa, implying dislocation densities between 10^8 and 10^{10} m^{-2}, would be sufficient to reproduce the plumes morphology observed in tomographic images.

1. Introduction

Mantle plumes are one of the modes of convection through which the Earth is cooling. As the Earth's mantle is at least partially heated from below, regions of hot and therefore less dense material can become unstable and rise (e.g., Schubert et al., 2001). Hot spot volcanism (Wilson, 1963) will result from the impact under the lithosphere of these hot instabilities (Morgan, 1971). In a homogeneous and Newtonian fluid, they take the shape of a mushroom (Figure 1), with a big head over a narrower stem (Griffiths & Campbell, 1990; Morgan, 1971; Sleep, 1990). On the Earth's surface, the hot head would produce traps while the stem would generate long volcanic tracks (Richards et al., 1989). Mantle plumes are therefore explaining first-order observations on a number of hot spots, as well as bringing up to us valuable information on the Earth's deep interior.

Seismically, these hot plumes should correspond to slow seismic velocity anomalies. Surface wave tomographic models have identified broad (~1,000 km) ponds of slow material down to 200 km depth beneath many hot spots (e.g., Debayle et al., 2005; Ritsema & Allen, 2003; Shapiro & Ritzwoller, 2002) as predicted by models of plume-lithosphere interactions (e.g., Olson, 1990; Ribe & Christensen, 1999; Sleep, 1990). Regional tomographic studies imaged low-velocity anomalies down to the transition zone beneath Afar (Debayle et al., 2001), Kenya (Chang & Van der Lee, 2011), Iceland (Rickers et al., 2013; Shen et al., 2002), the Eifel (Goes et al., 1999), Yellowstone (Schmandt et al., 2012), West Antartica (Hansen et al., 2014), Galapagos (Villagomez et al., 2007), and Hawaii (Wolfe et al., 2009, 2011). Studies using receiver functions show thinner transition zones beneath Cape Verde, Azores, Iceland, Society, Galapagos, and Hawaii, which may reflect the presence of a hot conduit (see Ballmer et al., 2015, for references). In the deeper mantle, short wavelength and slow anomalies are difficult to image because of wavefront healing effects (Nolet & Dahlen, 2000), the uneven distribution of earthquakes, and the lack of dense seismic networks, especially in the oceans. Therefore, the 100 to 200 km thick conduit predicted for the classical plume would not be resolved (French & Romanowicz, 2015; Nolet et al., 2006), and indeed, global tomography models could not detect continuous hot structures under hot spots for years. However, progress in tomography techniques has recently imaged continuous slow structures from the core-mantle boundary to the surface beneath about 10 hot spots (French & Romanowicz, 2015; Montelli et al., 2006; Zhao, 2001). Resolution analysis shows that most plumes would not be visible if their diameter was smaller than about 600 km (French & Romanowicz, 2015; Montelli et al., 2006). Indeed, the imaged plumes in finite frequency models PRI-S05 and PRI-P05 (Montelli et al., 2006) present diameters of at least 600–800 km. And waveform tomography model SEMUCB-WM1 (French & Romanowicz, 2015) recovers columnar structures with diameters 800 to 1,000 km (Figure 2). So hot plumes appear quite wide in the lower mantle, which is at odds with the common view of a hot plume morphology as a balloon head on a thin conduit.

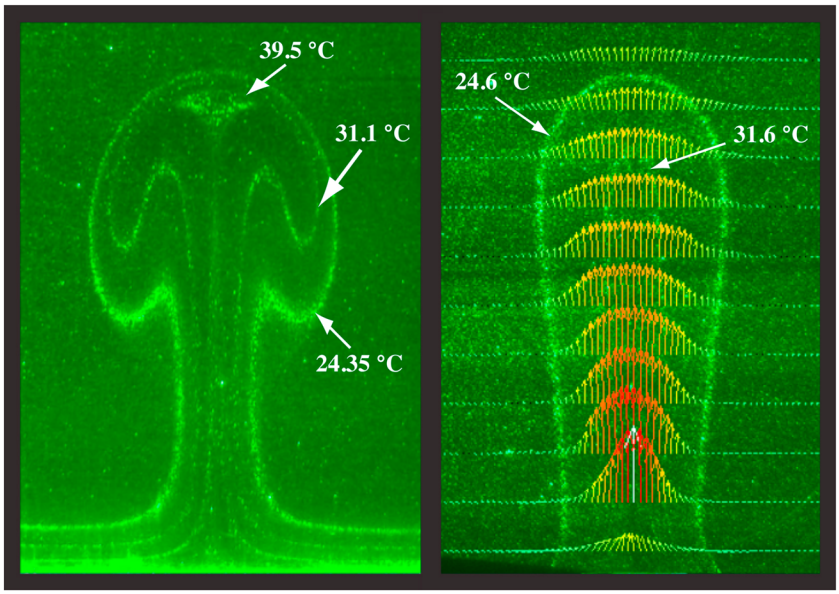

Figure 1. (left) Thermal plume in a Newtonian fluid (sugar syrup); the bright lines represents isotherms (experiment *lRa*12 from Androvandi et al., 2011). (right) Thermal plume in a yield stress fluid (Carbopol); on top of the isotherms (bright lines), the colored vectors show the velocity field (adapted from Davaille et al., 2013). Both set of experiments were run in a fluid initially at ambient temperature (21°C).

In a Newtonian homogeneous fluid, such a thick morphology would correspond either to a hot plume developing at much lower Rayleigh number than present-day mantle convection (Goes et al., 2004) or to a more viscous hot instability intruding in a less viscous mantle (Whitehead & Luther, 1975). It was pointed out that if diffusion creep was the main deformation mode in the lower mantle, the resulting strong increase of the viscosity with the crystal size, and the enhanced crystal growth rate with temperature, could produce hot plumes that are more viscous than the ambient mantle (e.g., Korenaga, 2005; Solomatov, 1996).

Another way to produce fat plume conduits in Newtonian fluids is to introduce compositional heterogeneities (Dannberg & Sobolev, 2015; Davaille et al., 2005; Kumagai et al., 2008; Lin & van Keken, 2006). Then the plume conduit can thicken due to thermo-compositional recirculation within the conduit itself (Kumagai et al., 2008).

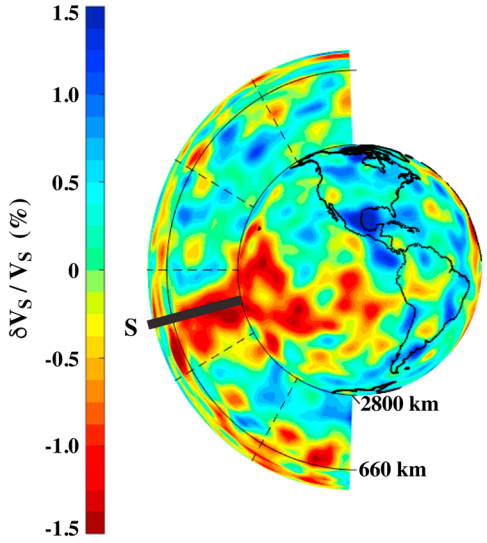

Figure 2. Samoa plume: Cross section of *S* seismic waves anomalies $\delta V_S/V_S$ (in ¸*percnt*;) below the Samoan hot spot (indicated by "S" on the Earth surface) in the tomographic model SEMUCB-WM1 of French and Romanowicz (2015). For comparison, the thick solid black line shows a conduit of 200 km diameter from 2,800 km depth to the surface.

We show here using recent laboratory experiments (Davaille et al., 2013; Massmeyer et al., 2013) that there is yet another avenue: thick hot thermal plumes could be produced in the lower mantle if the latter had a viscoplastic rheology, where flow occurs only when the local deviatoric stress becomes greater than a critical yield stress. As described in the following, such type of rheology could correspond to the one recently proposed for bridgmanite in the lower mantle by numerical modeling (Boioli et al., 2017). Section 2 presents the laboratory findings, while section 3 describes the occurrence of yield stresses in high-temperature creep mechanisms in the lower mantle. Section 4 discusses the implications for mantle plumes.

2. Fat Plumes in a Yield Stress Fluid

We recently studied experimentally the development of thermal plumes out of a localized heat source on the bottom of a tank filled with a Carbopol dispersion. The details of the studies can be found in Davaille et al. (2013) and in Massmeyer et al. (2013). A Carbopol dispersion is a polymeric fluid whose rheology can be described by a Hershel-Bulkley (hereafter "HB") law (e.g., Di Giuseppe et al., 2015; Piau, 2007). When the stress σ exceeds a critical value σ_0, called yield stress, shear thinning occurs with

$$\sigma = \sigma_0 + K_v \dot{\gamma}^{n_{HB}} \quad (1)$$

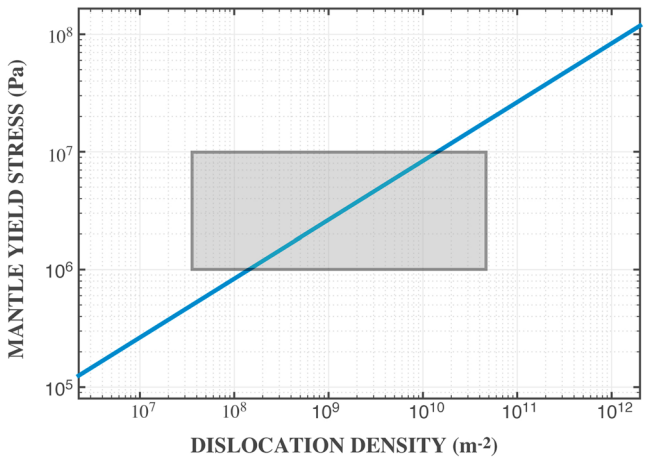

Figure 3. Typical dislocation density dependence of the threshold stress for bridgmanite. In equation (4), we use $G = 180$ GPa (Matas et al., 2007), $b = 0.465$ nm, and $\beta = 1$ (e.g., Boioli et al., 2017).

where $\dot{\gamma}$ is the shear rate, K_v is the consistency, and n_{HB} is an exponent between 0.3 and 0.75. So when motions occur, an effective viscosity can be defined for the fluid

$$\eta = \sigma/\dot{\gamma} = \sigma_0 \dot{\gamma}^{-1} + K_v \dot{\gamma}^{n_{HB}-1} \quad (2)$$

Note that the last member of this equation is similar to a dislocation creep where the shear thinning exponent would be $n = 1/n_{HB}$. When local stresses are smaller than σ_0, the HB model assumes that deformation is zero (e.g., Piau, 2007). In a real material, this is not true, and thermo-elastic stresses have to be considered (e.g., Sgreva & Davaille, 2017).

To describe the system dynamics, the key parameter is the "yield parameter" Y_0, which compares the thermally induced stress to the yield stress. Three different regimes are observed. For low Y_0, no convection develops and deformation is purely elastic. For intermediate Y_0 values, the thermo-elastic stresses generated by heating are big enough to overcome the yield stress: a convection cell appears but remains confined around the heater. For high Y_0, the stresses generated by the thermal buoyancy of the hot pocket around the heater become much larger than the yield stress and a thermal plume develops (Figure 1). Its morphology differs from the mushroom shape typically encountered in Newtonian fluids. Combined temperature and velocity field measurements show that a plug flow develops within the plume thermal anomaly and that deformation is strongly localized on its edges. This produces a rising finger shape (Figure 1). Scaling analysis (Davaille et al., 2013; Massmeyer et al., 2013) shows that plume uplift occurs when

$$Y_0 = \frac{gD\Delta\rho}{\sigma_0} > Y_c = 15 \pm 3.6 \quad (3)$$

where D is the plume diameter, the density difference between the plume and the ambient fluid is $\Delta\rho = \alpha\rho\Delta T_{av}$, α is thermal expansion, and ΔT_{av} is the averaged temperature excess of the plume compared to the ambient fluid. Fat plumes were observed in the laboratory up to $Y_0 \sim 10Y_c$.

3. On Yield Stresses During High-Temperature Creep in the Mantle

The existence (or not) of a yield stress depends on the microstructure of the fluid and the way motion is activated. Our Carbopol solutions are polymeric gels constituted of elastic micron-scale sponges that aggregate and jam. So the yield stress comes from the fact that the microstructure at first resists deformation (Oppong, 2011; Piau, 2007).

In mantle rocks, the yield stress or elastic limit of a crystal is not an intrinsic characteristics, but depends on its defects microstructure. Moreover, the development of a given microstructure is a direct consequence of the mechanism involved during the creep regime. Two processes are commonly considered to account for flow in the mantle: diffusion creep and dislocation creep.

In diffusion creep, strain results directly from the motion of crystal point defects. Since the vacancy concentration close to a grain boundary under tension is greater than that close to a grain boundary under compression, a net flux of matter develops from sources to sinks. At high temperatures, vacancies can diffuse through the bulk of the grain (the Nabarro-Herring creep mechanism) or along the grain boundaries (Coble mechanism). The efficiency of both mechanism is limited by the grain size, which conditions the characteristic distance between sources and sinks (Poirier, 1985). Even before diffusion creep was actually observed experimentally, Nabarro and Herring proposed theoretically a constitutive equation for this process: the main characteristic of diffusion creep is that it is Newtonian viscous ($\sigma \sim \dot{\gamma}$) and grain size dependent. Hence, there would be no yield stress associated with Nabarro-Herring creep.

In dislocation creep, strain is produced by the glide of a fraction of the dislocations that are made free to move owing to two thermally activated recovery mechanisms: cross slip whereby screw dislocations deviate from their initial glide plane, and climb where nonscrew dislocations move out of the glide planes after absorbing

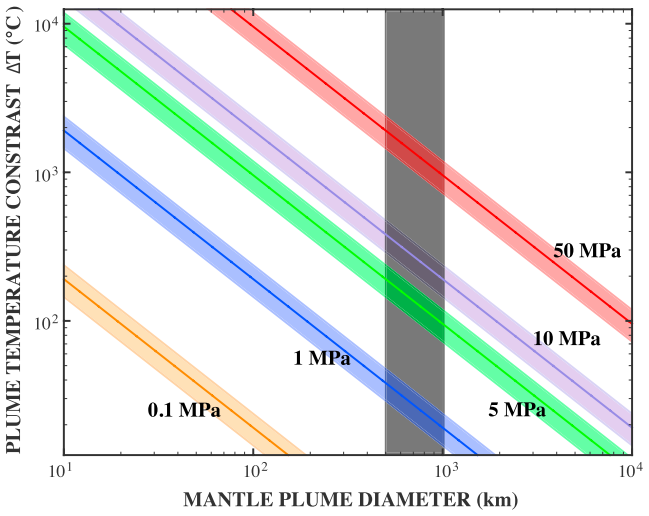

Figure 4. Yield stress allowing the development of fat plumes in the lower mantle as a function of plume temperature anomaly and radius. The dark box outlines the mantle fat plumes domain.

point defects (Poirier, 1985). Frank proposed that dislocations distributed at random among several slip systems form a three-dimensional network that has a characteristic dimension that scales like $l = \rho_d^{-1/2}$, where ρ_d is the dislocation density (see, for instance, Friedel, 1964). The yield stress can be related to the stress necessary to create new dislocations by activating dislocation sources from dislocations segments of the Frank network. Also, any mobile dislocation will have to overcome the long range elastic stresses produced by the network or the short-range interactions due to crossing with the dislocations of the Frank network. All these mechanisms define a critical stress that scales with

$$\sigma_y \propto \frac{Gb}{\beta l} = \frac{1}{\beta} Gb\rho_d^{1/2} \tag{4}$$

where G is the shear modulus, b the modulus of the Burgers vector, and β is a numerical constant of the order of 1–5 depending on the nature of the interactions (Friedel, 1964). Hence, the yield stress comes from the jammed nature of the population of dislocations. Figure 3 shows how the threshold stress increases as a function of the dislocation density.

In the meantime, we can use the scaling law (equation (3)) to estimate the yield stress (Figure 4) required to generate fat plumes in the mantle as imaged by the recent global tomographic models (Figure 2; French & Romanowicz, 2015; Montelli et al., 2006). Figure 4 shows that yield stresses values between 1 and 10 MPa would allow plumes with diameters ranging from 600 to 1,000 km and averaged temperature anomalies of 50 to 800°C to develop. According to equation (4) and Figure 3, such yield stress estimates would imply dislocation densities between 10^8 and 10^{10} m^{-2}.

4. Discussion and Conclusions

In the previous section, we showed that the dislocation creep mechanism in a crystal always implies the existence of a yield stress scaling on the dislocation density of the crystal. Recent numerical simulations have shown that under pressure and temperature conditions of the lower mantle, dislocation glide is extremely difficult in bridgmanite (Kraych et al., 2016), even under mantle strain rates. Standard dislocation creep involving glide and climb can thus no longer be considered. However, Boioli et al. (2017) have demonstrated that dislocation climb can provide an alternative deformation mechanism. Plastic strain is then produced by dislocation climb induced by emission and absorption of vacancies. The dislocations inside the grains thus play the role of sources and sinks for vacancy diffusion. By introducing a characteristic distance for diffusion smaller than the grain size, pure climb creep is grain size independent, and it is more efficient than the standard Nabarro-Herring (or Coble) creep features (Boioli et al., 2017). It is also worth noticing that even in case of pure climb creep, dislocation multiplication will only occur for stresses higher than the yield stress σ_y. Boioli et al. (2017) further showed that dislocation densities between 10^8 and 10^{10} m^{-2} (i.e., section 3) are sufficient to produce deformation at strain rates that correspond to our best estimates of those in the lower mantle ($10^{-14} - 10^{-16}$ s^{-1}).

Moreover, since pure climb creep involves no lattice rotation, it does not produce crystal lattice preferred orientation. This could explain why seismic anisotropy has not been detected in most of the lower mantle. The weak anisotropy reported below 2,000 km depths (e.g., De Witt & Trampert, 2015; Montagner & Kennett, 1996) and the strong azimuthal anisotropy observed in the D'' layer at the bottom of the mantle (e.g., De Witt & Trampert, 2015; Montagner & Kennett, 1996; Panning & Romanowicz, 2004) would then be due to different minerals (post-perovskite and magnesiowustite) or to the alignment of materials with differing elastic properties through shape-preferred orientation.

The existence of a critical yield stress in the rheology would also have important implications for mantle stirring and mixing. As already seen in section 2, such a rheology strongly localizes motions and shear, while "dead zones" develop in the remaining fluid. Their existence might strongly impede mantle stirring efficiency, leading to the long-term preservation of primitive material. More work is in progress to study this problem quantitatively.

Nevertheless, we demonstrate here that microstructural parameters such as dislocation microstructures at the submillimeter scale can have implications on large-scale processes and features. Unfortunately, compared to other deformations modes, very few studies (especially involving microstructural characterization) have been devoted to materials deforming by pure climb creep (the study of Beauchesne & Poirier, 1990 on $KNbO_3$ perovskite is one of those). Hence, our knowledge on how dislocation microstructures develop during pure climb creep, and how they respond to loading conditions is too limited. It seems important to carry on such studies in the future to better constrain the rheology of bridgmanite and therefore the rheology of the lower mantle.

Acknowledgments
The laboratory experiments have been supported by French ANR PTECTO and CNRS/INSU/CNES Programme de Planetologie. The numerical simulations of the mantle creep have been supported by funding from the European Research Council under the Seventh Framework Programme (FP7), ERC grant 290424 - Rheoman. The data used are listed in the references. We thank the Editor and an anonymous reviewer for their comments on the manuscript.

References

Androvandi, S., Davaille, A., Limare, A., Fouquier, A., & Marais, C. (2011). At least three scales of convection in a mantle with strongly temperature-dependent viscosity. *Physics of the Earth and Planetary Interiors*, *188*, 132–141.

Ballmer, M. D., Ito, G., & van Keken, P. (2015). Hotspots, large igneous provinces and melting anomalies. In G. Schubert & D. Bercovici (Eds.), *Mantle dynamics* (2nd ed., pp. 393–459). Elsevier, Treatise of Geophysics 7.10.

Beauchesne, S., & Poirier, J.-P. (1990). In search of a systematics for the viscosity of perovskites: Creep of potassium tantalate and niobate. *Physics of the Earth and Planetary Interiors*, *61*, 182–198.

Boioli, F., Carrez, Ph., Cordier, P., Devincre, B., Gouriet, K., Hirel, P., et al. (2017). Pure climb creep mechanism drives flow in Earth's lower mantle. *Science Advances*, *3*, E1601958.

Chang, S-J., & Van der Lee, S. (2011). Mantle plumes and associated flow beneath Arabia and East Africa. *Earth and Planetary Science Letters*, *302*, 448–454.

Dannberg, J., & Sobolev, S. V. (2015). Low-buoyancy thermochemical plumes resolve controversy of classical mantle plume concept. *Nature Communications*, *6*, 6960. https://doi.org/10.1038/ncomms7960

Davaille, A., Gueslin, B., Massmeyer, A., & Di Giuseppe, E. (2013). Thermal instabilities in yield stress fluids: Existence and morphology. *Journal of Non-Newtonian Fluid Mechanics*, *193*, 144–153.

Davaille, A., Stutzmann, E., Silveira, G., Besse, J., & Courtillot, V. (2005). Convective patterns under the Indo-Atlantic "box". *Earth and Planetary Science Letters*, *239*, 233–252.

Debayle, E., Kennett, B., & Priestley, K. (2005). Global azimuthal seismic anisotropy and the unique plate motion deformation of Australia. *Nature*, *433*, 509–512.

Debayle, E., Leveque, J.-J., & Cara, M. (2001). Seismic evidence for a deeply rooted low-velocity anomaly in the upper mantle beneath the northeastern Afro/Arabian continent. *Earth and Planetary Science Letters*, *193*, 369–382.

Di Giuseppe, E., Corbi, F., Funiciello, F., Massmeyer, A., Santimano, T. N., Rosenau, M., & Davaille, A. (2015). Characterization of Carbopol hydrogel rheology for experimental tectonics and geodynamics. *Tectonophys*, *642*, 29–45.

De Witt, R. W. L., & Trampert, J. (2015). Robust constraints on average radial lower mantle anisotropy and consequences for composition and texture. *Earth and Planetary Science Letters*, *429*, 1001–109.

French, S. W., & Romanowicz, B. (2015). Broad plumes rooted at the base of the Earth's mantle beneath major hotspots. *Nature*, *525*, 95–99.

Friedel, J. (1964). *Dislocations*. Oxford: Pergamon Press.

Goes, S., Cammarano, F., & Hansen, U. (2004). Synthetic seismic signature of thermal mantle plumes. *Earth and Planetary Science Letters*, *218*, 403–419.

Goes, S., Spakman, W., & Bijwaard, H. (1999). A lower mantle source for central European volcanism. *Science*, *286*, 1928–1931.

Griffiths, R. W., & Campbell, I. H. (1990). Stirring and structure in mantle starting plumes. *Earth and Planetary Science Letters*, *99*, 66–78.

Hansen, S. E., Graw, J. H., Kenyon, L. M., Nyblade, A. A., Wiens, D. A., Aster, R. C., et al. (2014). Imaging the Antarctic mantle using adaptively parameterized P-wave tomography: Evidence for heterogeneous structure beneath West Antarctica. *Earth and Planetary Science Letters*, *408*, 66–78.

Korenaga, J. (2005). Firm mantle plumes and the nature of the core-mantle boundary region. *Earth and Planetary Science Letters*, *232*, 29–37.

Kraych, A., Carrez, Ph., & Cordier, P. (2016). On dislocation glide in $MgSiO_3$ bridgmanite at high-pressure and high-temperature. *Earth and Planetary Science Letters*, *452*, 60–68.

Kumagai, I., Davaille, A., Kurita, K., & Stutzmann, E. (2008). Mantle plumes: Thin, fat, successful, or failing? Constraints to explain hot spot volcanism through time and space. *Geophysical Research Letters*, *35*, L16301. https://doi.org/10.1029/2008GL035079

Lin, S.-C., & van Keken, P. E. (2006). Dynamics of thermochemical plumes: 1. Plume formation and entrainment of a dense layer. *Geochemistry, Geophysics, Geosystems*, *7*, Q02006. https://doi.org/10.1029/2005GC001071

Matas, J., Bass, J., Ricard, Y., Mattern, E., & Bukowinski, M. S. T. (2007). On the bulk composition of the lower mantle: Predictions and limitations from generalized inversion of radial seismic profiles. *Geophysical Journal International*, *170*, 764–780.

Massmeyer, A., Di Giuseppe, E., Davaille, A., Rolf, T., & Tackley, P. J. (2013). Numerical simulation of thermal plumes in a Herschel–Bulkley fluid. *Journal of Non-Newtonian Fluid Mechanics*, *195*, 32–45.

Montagner, J.-P., & Kennett, B. L. N. (1996). How to reconcile body-wave and normal-mode reference Earth models.*Geophysical Journal International*, *125*, 229–248.

Montelli, R., Nolet, G., Dahlen, F. A., & Masters, G. (2006). A catalogue of deep mantle plumes: New results from finite-frequency tomography. *Geochemistry, Geophysics, Geosystems*, *7*, Q11007. https://doi.org/10.1029/2006GC001248

Morgan, W. J. (1971). Convection plumes in the lower mantle. *Nature*, *230*, 42–43.

Nolet, G., & Dahlen, F. A. (2000). Wavefront healing and the evolution of seismic delay times. *Journal of Geophysical Research*, *105*, 19043–19054.

Nolet, G., Karato, S.-i., & Montelli, R. (2006). Plume fluxes from seismic tomography. *Earth and Planetary Science Letters*, *248*, 685–699.

Panning, M., & Romanowicz, B. (2004). Inference on flow at the base of Earth's mantle based on seismic anisotropy. *Science*, *303*, 351–353.

Olson, P. (1990). Hot spots, swells and mantle plumes. In M. P. Ryan (Ed.), *Magma transport and storage* (pp. 33–51). New York: John Wiley and Sons.

Oppong, F. (2011). Microrheology and jamming in a yield stress fluid. *Rheologica Acta*, *50*, 317–326.

Piau, J. M. (2007). Carbopol gels: Elastoviscoplastic and slippery glasses made of individual swollen sponges: Meso- and macroscopic properties, constitutive equations and scaling laws. *Journal of Non-Newtonian Fluid Mechanics*, *144*, 1–29.

Poirier, J.-P. (1985). *Creep of crystals: High-temperature deformation processes in metals, ceramics and minerals*. New York: Cambridge University Press.

Ribe, N. M., & Christensen, U. R. (1999). The dynamical origin of Hawaiian volcanism. *Earth and Planetary Science Letters*, *171*, 517–531.
Richards, M. A., Duncan, R. A., & Courtillot, V. E. (1989). Flood basalts and hotspot tracks: Plume heads and tails. *Science*, *246*, 103–107.
Rickers, F., Fichtner, A., & Trampert, J. (2013). The Iceland-Jan Mayen plume system and its impact on mantle dynamics in the North Atlantic region: Evidence from full-waveform inversion. *Earth and Planetary Science Letters*, *367*, 39–51.
Ritsema, J., & Allen, R. M. (2003). The elusive mantle plume. *Earth and Planetary Science Letters*, *207*, 1–12.
Schmandt, B., Dueker, K., Humphreys, E., & Hansen, S. (2012). Hot mantle upwelling across the 660 beneath Yellowstone. *Earth and Planetary Science Letters*, *331*, 224–236.
Schubert, G., Turcotte, D. L., & Olson, P. (2001). *Mantle convection in the Earth and planets*. Cambridge: Cambridge University Press, p. 940.
Sgreva, N. R., & Davaille, A. (2017). *Influence of the thermo-elastic stresses on the onset of convective motion in Carbopol, VPF2017*. Rotorua, NZ: Viscoplastic Fluids Workshop: From Theory to Applications.
Shapiro, N. M., & Ritzwoller, M. H. (2002). Monte-Carlo inversion for a global shear-velocity model of the crust and upper mantle. *Geophysical Journal International*, *151*, 88–105.
Shen, Y., Solomon, S. C., Bjarnason, I. T., Nolet, G., Morgan, W. J., Allen, R. M., et al. (2002). Seismic evidence for a tilted mantle plume and north-south mantle flow beneath Iceland. *Earth and Planetary Science Letters*, *197*, 261–272.
Sleep, N. H. (1990). Hotspots and mantle plumes: Some phenomenology. *Journal of Geophysical Research*, *95*, 6715–6736.
Solomatov, V. S. (1996). Can hotter mantle have a larger viscosity? *Geophysical Research Letters*, *23*, 937–940.
Villagomez, D., Toomey, D. R., Hooft, E. E. E., & Solomon, S. C. (2007). Upper mantle structure beneath the Galapagos Archipelago from surface wave tomography. *Journal of Geophysical Research*, *112*, B07303. https://doi.org/10.1029/2006JB004672
Whitehead, J. A., & Luther, D. S. (1975). Dynamics of laboratory diapir and plume models. *Journal of Geophysical Research*, *80*, 705–717.
Wilson, J. T. (1963). A possible origin of the Hawaiian Islands. *Canadian Journal of Physics*, *41*, 863–870.
Wolfe, C. J., Solomon, S. C., Laske, G., Collins, J. A., Detrick, R. S., Orcutt, J. A., et al. (2009). Mantle shear-wave velocity structure beneath the Hawaiian hot spot. *Science*, *326*, 1388–1390.
Wolfe, C. J., Solomon, S. C., Laske, G., Collins, J. A., Detrick, R. S., Orcutt, J. A., et al. (2011). Mantle *P*-wave velocity structure beneath the Hawaiian hotspot. *Earth and Planetary Science Letters*, *303*, 267–280.
Zhao, D. (2001). Seismic structure and origin of hotspots and mantle plumes. *Earth and Planetary Science Letters*, *192*, 251–265.